Int. J. Heat Mass Transfer. Vol. 32, No. 4, pp. 751–760, 1989
Printed in Great Britain

0017–9310/89 $3.00 + 0.00

The contact heating and lubricating flow of a body of glass

ADRIAN BEJAN and PEDRO A. LITSEK
Department of Mechanical Engineering and Materials Science, Duke University, Durham, NC 27706, U.S.A.

(*Received* 29 *April* 1988 *and in final form* 1 *September* 1988)

Abstract—This paper describes analytically the process in which a body of glass is heated, softened and eroded ('melted' away) by direct contact with a solid surface of much higher temperature. This surface can slide relative to the body of glass. The glass is modelled as a liquid the viscosity of which varies as T^{-n}, where T is the absolute temperature and n is a number in the range 10–20. The temperature and velocity distributions in the thin layer of hot (soft) glass are determined. Simple calculation procedures are developed for the rate at which the block of glass is eroded, and for the general relationship between the forces exerted on the block and the combined heat transfer and lubrication phenomenon that governs the glass removal process.

1. INTRODUCTION

THE OBJECTIVE of this paper is to describe the most fundamental features of the process by which a body of glass is superficially heated, softened and eroded by the contact with a solid object of higher temperature. The solid object (heater) can also slide relative to the body of glass, that is in the direction parallel to the surface of contact (Fig. 1). The engineering objective of the analysis is to uncover the relationship between the force with which the glass block is pressed against the heater surface, and the apparent 'melting' speed with which the block advances downward toward the heater.

The process considered in this paper is one in which the obvious heat transfer problem is intimately coupled with a fluid mechanics 'lubrication' problem, in such a way that the force that is exerted on the block drives the flow of the soft glass generated in the layer adjacent to the heater. This combined heat transfer and lubrication problem is related to the problem of close-contact melting, which has been treated by Moallemi and Viskanta [1, 2], Webb *et al.* [3] and Bareiss and Beer [4]. In the melting problem, a thin film of liquid separates the heater from the block of the solid phase-change material. The liquid serves as lubricant and is generated steadily across a sharp two-phase interface.

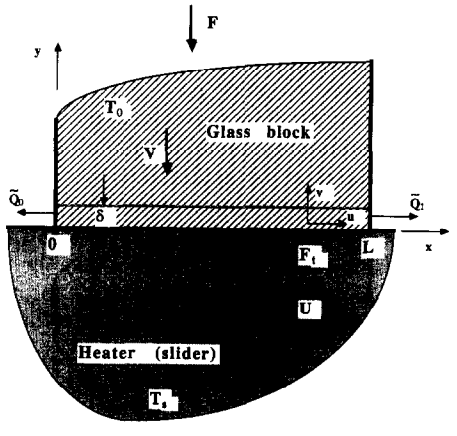

FIG. 1. Body of glass pushed against the flat surface of a sliding heater.

In the present problem, the sharp two-phase interface does not exist: the block of glass remains single phase (liquid). The effect of the bottom heater is to drastically decrease the viscosity of glass in a thin layer in the vicinity of the contact surface. The layer of soft glass acts as lubricant for the relative motion between the heater and the body of room-temperature glass. The latter appears 'hard' to the touch because close to room temperature its viscosity is enormous (e.g. Fig. 3). Put another way, in the following analysis the glass material is treated as a newtonian liquid the viscosity of which decreases dramatically as the temperature increases.

2. THE PHYSICAL MODEL

Consider the heat transfer configuration shown in Fig. 1. A two-dimensional block of glass (the shaded material) is being pressed against a flat isothermal solid of temperature T_s. Sufficiently far above the region of contact, the temperature of the glass body is equal to the ambient temperature T_0. The system of coordinates x–y is attached to the leading edge of the glass body and the horizontal interface. In this frame of reference, the base solid moves to the right with the velocity U.

We focus on the steady process in which the glass body is heated in a boundary layer region (δ) by the thermal contact with the base solid. This heating effect

NOMENCLATURE

B characteristic dimensionless group, equation (30)
c specific heat of glass
F normal force, equation (35) [N m^{-1}]
$\tilde{F}$ dimensionless normal force, equation (44)
F_t tangential force, equation (48) [N m^{-1}]
$\tilde{F}_t$ dimensionless tangential force, equation (49)
I_0, I_1, I_2, I_3 integrals defined in equations (16), (17), (25) and (26), respectively
k thermal conductivity of glass
L length of contact surface
n exponent in the power-law viscosity model, equation (3)
P pressure
$\tilde{P}$ dimensionless pressure, equation (14)
Pe Peclet number, UL/α_0
$\tilde{Q}$ dimensionless longitudinal flow rate, equation (22)
T absolute temperature
u, v velocity components, Fig. 1
$\tilde{u}$ dimensionless longitudinal velocity, u/U
U relative horizontal velocity between glass block and heater (slider), Fig. 1
V downward velocity, or rate of glass erosion, Fig. 1
x, y Cartesian coordinates, Fig. 1
$\tilde{y}$ dimensionless transversal coordinate, equation (9)
Y dimensionless transversal coordinate, y/L
Y_∞ distance larger than δ.

Greek symbols
α thermal diffusivity
β dummy variable
δ thermal boundary layer thickness, $k_0/(\rho c V)$
ε room temperature limit parameter, equation (20)
η function, equation (40)
μ viscosity
ξ dimensionless longitudinal coordinate, x/L
ρ density
τ dimensionless temperature, T/T_0
ϕ function, equation (37)
ϕ_r value of ϕ when $\varepsilon = 0.01$, Fig. 4.

Subscripts
0 property evaluated at room temperature
s property evaluated at the heater temperature.

induces a softening of the glass in the δ-thin layer. The soft glass is squeezed out through both ends of the contact region, as the block of glass is pressed vertically downward with the total force F. In order to replenish the glass that is steadily squeezed out of the δ-thin region, the glass body advances downward with the velocity V. The engineering objective of this study is to determine the relationship between the rate of glass removal (V), the applied force (F) and the other dimensions and physical properties of the heat transfer arrangement.

In order to be able to make some analytical progress on this problem (that is, before resorting to numerical analysis), we adopt the following assumptions. First, we model the softened glass as a material with thermal conductivity proportional to the local absolute temperature

$$k = k_0 \tau \tag{1}$$

where

$$\tau = \frac{T}{T_0} \tag{2}$$

and (T_0, k_0) are glass properties at the environmental state. Figure 2 and the thermal conductivity data of ref. [5] show that equation (1) represents adequately the shape of the empirical $k(T)$ function in the high temperature range ($T \sim 10^3$ K) where glasses flow.

The second assumption consists of writing a power law expression for the viscosity of glass

$$\mu = \mu_0 \tau^{-n}. \tag{3}$$

Figure 3 and the viscosity data collected from ref. [6] show that equation (3) is particularly appropriate in the high temperature range. For most soda-lime glasses at temperatures of the order of 10^3 K, the exponent n is typically of the order of 10 or 20. The room-temperature viscosity μ_0 is not furnished by experiments, because close to room temperature glass behaves as an elastic amorphous material. Therefore, the constant μ_0 must be determined by first fitting equation (3) to the high-temperature end of the experimentally measured $\mu(T)$ curve, and then by extending that line all the way to $T = T_0$. Note that the same procedure is required in order to determine the room-temperature conductivity k_0 that is to be used in equation (1).

The third assumption is that the thermal boundary layer thickness δ is constant (independent of x), or that the temperature distribution in that layer is a function of y only. This description is a good one in the case of thermal boundary layers of the 'stagnation

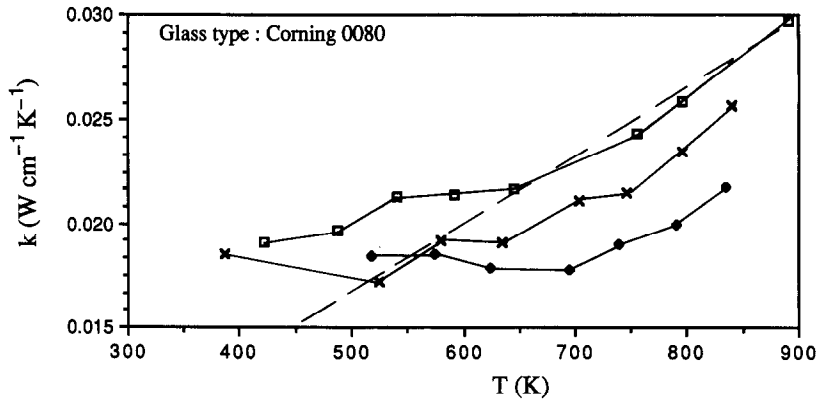

FIG. 2. Illustrations of the temperature dependence of the thermal conductivity of glass. The different sets of data correspond to different samples of the same glass type (Corning 0080) [11].

flow' type. For example, from the study of natural convection horizontal boundary layers on cold plates facing upward [7, 8], we know to expect the formation of a thermal boundary layer of almost constant thickness over most of the plate length L. Furthermore, in an analog of the present two-dimensional problem, in which the glass body is replaced by a block of phase-change material with definite melting point [9], it was found that the contact region is occupied by a very thin liquid layer (melt) of constant thickness. The two-dimensionality of the geometry of Fig. 1 appears to be important vis-à-vis the validity of the constant-δ assumption, because in the melting of a radially symmetric (cylindrical) block of phase-change material Saito *et al.* [10] found that the thickness of the liquid layer is not uniform.

In the problems of refs. [7–9] (and, particularly, in the present one) the constant-δ approximation breaks down in the vicinity of the two ends, $x = 0$ and L. However, the ends are the very regions in which the classical lubrication theory (Section 4) breaks down anyway. We return to this observation in the concluding section of the paper.

3. THE TEMPERATURE DISTRIBUTION

The flow of the heated glass depends greatly on the viscosity that the heated layer achieves while in contact with the base surface. In turn, the viscosity depends on the temperature reached by the thermal boundary layer. We can determine the temperature distribution analytically by solving the energy equation

$$\rho c\left(u\frac{\partial T}{\partial x}+v\frac{\partial T}{\partial y}\right)=\frac{\partial}{\partial x}\left(k\frac{\partial T}{\partial x}\right)+\frac{\partial}{\partial y}\left(k\frac{\partial T}{\partial y}\right) \quad (4)$$

in which the specific heat capacity (ρc) is a known constant. According to the third assumption made in the preceding section we recognize that $T = T(y)$ over most of the contact length, therefore, equation (4) reduces to

$$\rho c v\frac{\partial T}{\partial y}=\frac{\partial}{\partial y}\left(k\frac{\partial T}{\partial y}\right). \quad (5)$$

The vertical velocity v decreases from $v = -V$ at the outer edge of the boundary layer to $v = 0$ at the impermeable base surface, $y = 0$. In order to decouple the energy equation (5) from the fluid mechanics part of the problem (Section 4), we assume that $v = -V$ throughout the boundary layer region to which equation (5) applies. Consequently, equation (5) can be integrated twice in y, and the result is the exponential temperature distribution given implicitly by

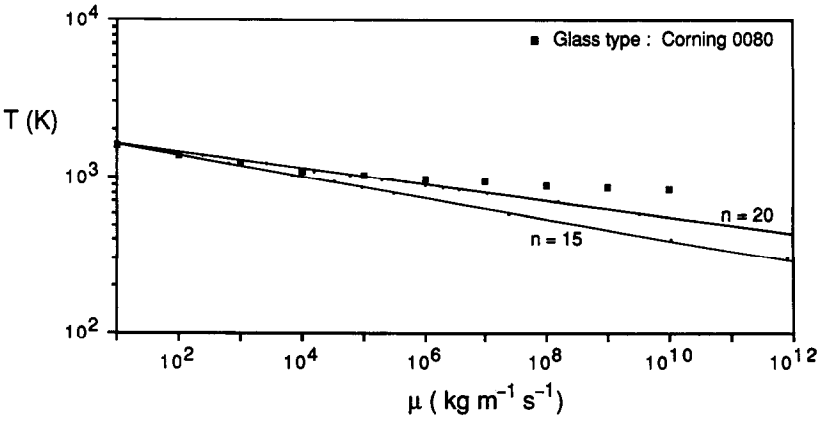

FIG. 3. Illustrations of the temperature dependence of the viscosity of glass.

$$\tilde{y} = \tau_s - \tau + \ln\frac{\tau_s - 1}{\tau - 1}. \quad (6)$$

The path from equation (5) to equation (6) consists of using also the known temperature boundary conditions

$$\tau = \tau_s \quad \text{at} \quad \tilde{y} = 0 \quad (7)$$

$$\tau \to 1 \quad \text{as} \quad \tilde{y} \to \infty. \quad (8)$$

The dimensionless vertical coordinate $\tilde{y}$ is defined as

$$\tilde{y} = y\frac{\rho c V}{k_0} \quad (9)$$

in other words, the thermal boundary layer thickness δ varies as $k_0/(\rho c V)$. The thermal boundary layer becomes thinner as the vertical feed velocity V increases.

4. THE LONGITUDINAL FLOW

We now turn our attention to the flow of the heated glass layer along the base surface. The chief assumption on which the fluid mechanics part of this treatment is based is the same as in Osborne Reynolds' classical theory of film lubrication (see, e.g. Batchelor [12]). The heated glass layer is assumed to be sufficiently slender so that the effect of inertia is negligible in the boundary layer-simplified momentum equation. For this we write

$$\frac{dP}{dx} = \frac{\partial}{\partial y}\left[\mu\frac{\partial u}{\partial y}\right] \quad (10)$$

in which the pressure P depends only on x in the heated glass layer. In view of viscosity model (3), momentum equation (10) can be nondimensionalized as

$$\frac{d\tilde{P}}{d\xi} = \frac{\partial}{\partial\tilde{y}}\left(\tau^{-n}\frac{\partial\tilde{u}}{\partial\tilde{y}}\right) \quad (11)$$

in which the new dimensionless variables are

$$\xi = \frac{x}{L} \quad (12)$$

$$\tilde{u} = \frac{u}{U} \quad (13)$$

$$\tilde{P} = \frac{P}{\mu_0 UL}\left(\frac{k_0}{\rho c V}\right)^2. \quad (14)$$

The solution for the longitudinal velocity distribution $\tilde{u}$ is obtained by eliminating $\tilde{y}$ between equations (11) and (6), and then integrating the resulting equation twice in τ

$$\tilde{u} = I_1(\tau,\tau_s)\frac{d\tilde{P}}{d\xi} - C_1 I_0(\tau,\tau_s) + C_2. \quad (15)$$

The functions I_0 and I_1 are shorthand for two integrals the values of which are always positive

$$I_0(\tau,\tau_s) = \int_\tau^{\tau_s}\frac{\beta^{n+1}}{\beta-1}\,d\beta \quad (16)$$

$$I_1(\tau,\tau_s) = \int_\tau^{\tau_s}\left(\tau_s - \beta + \ln\frac{\tau_s-1}{\beta-1}\right)\frac{\beta^{n+1}}{\beta-1}\,d\beta. \quad (17)$$

The constants of integration C_1 and C_2 follow from the two boundary conditions on $\tilde{u}$, namely, the no-slip condition along the base

$$\tilde{u} = 1 \quad \text{at} \quad \tau = \tau_s \quad (18)$$

and the statement that the motion of the glass body is purely vertical outside the boundary layer

$$\tilde{u} \to 0 \quad \text{as} \quad \tau \to 1. \quad (19)$$

However, since $\beta > 1$ and the integrands of both I_0 and I_1 blow up at the point where $\beta = 1$ exactly, we replace boundary condition (19) with

$$\tilde{u} \to 0 \quad \text{at} \quad \tau = 1+\varepsilon \quad (20)$$

in which ε is a number much smaller than 1. We show later that the choice of ε has a negligible effect on the chief conclusion of this study, namely, the relationship between the applied force and the glass removal rate V. In conclusion, by combining equation (15) with the constants determined from equations (18) and (20) we obtain the longitudinal velocity distribution

$$\tilde{u} = \left[I_1(\tau,\tau_s) - I_0(\tau,\tau_s)\frac{I_1(1+\varepsilon,\tau_s)}{I_0(1+\varepsilon,\tau_s)}\right]\frac{d\tilde{P}}{d\xi} - \frac{I_0(\tau,\tau_s)}{I_0(1+\varepsilon,\tau_s)} + 1. \quad (21)$$

The velocity distribution $\tilde{u}$ derived above is a function of the longitudinal position (ξ), the transversal position (τ) and the temperature extremes bridged by the boundary layer (τ_s and $1+\varepsilon$). A result that can be calculated from equation (21) is the local longitudinal flow rate through the heated glass layer

$$\tilde{Q} = \int_0^\infty \tilde{u}\,d\tilde{y}. \quad (22)$$

In view of equation (6), the above definition is equivalent to

$$\tilde{Q} = \int_{\tau_s}^{1+\varepsilon}\tilde{u}(\xi,\beta,\varepsilon,\tau_s)\frac{\beta}{1-\beta}\,d\beta \quad (23)$$

which shows more clearly that $\tilde{Q}$ depends on ξ, ε, and τ_s. Combining equations (21) and (23) yields finally

$$\tilde{Q}(\xi,\varepsilon,\tau_s) = \frac{d\tilde{P}}{d\xi}I_3(1+\varepsilon,\tau_s) + I_2(1+\varepsilon,\tau_s) \quad (24)$$

in which I_2 and I_3 denote the integrals

$$I_2(1+\varepsilon,\tau_s) = \int_{1+\varepsilon}^{\tau_s}\left[1 - \frac{I_0(\beta,\tau_s)}{I_0(1+\varepsilon,\tau_s)}\right]\frac{\beta}{\beta-1}\,d\beta \quad (25)$$

$$I_3(1+\varepsilon,\tau_s)=\int_{1+\varepsilon}^{\tau_s}\left[I_1(\beta,\tau_s)-I_0(\beta,\tau_s)\frac{I_1(1+\varepsilon,\tau_s)}{I_0(1+\varepsilon,\tau_s)}\right]\times\frac{\beta}{\beta-1}\,d\beta. \quad (26)$$

The longitudinal flow rate $\tilde{Q}$ depends on the temperature extremes through I_2 and I_3, and on the longitudinal position through the still undetermined pressure distribution $\tilde{P}$.

5. THE PRESSURE DISTRIBUTION

The concluding step in this method of solution consists of integrating equation (24) once in ξ, in order to find the pressure $\tilde{P}$. We can execute this step by first determining the longitudinal flow rate function $\tilde{Q}$. The conservation of mass in two-dimensional incompressible flow requires

$$\frac{\partial u}{\partial x}+\frac{\partial v}{\partial y}=0 \quad (27)$$

which, integrated from $y=0$ to a distance Y_∞ outside the heated boundary layer region yields

$$\frac{d}{dx}\int_0^{Y_\infty}u\,dy=V. \quad (28)$$

The dimensionless counterpart of this result is obtained by using equations (12), (13) and (22)

$$\frac{d\tilde{Q}}{d\xi}=B \quad (29)$$

in which B is the dimensionless parameter that is being sought in this problem (note that if we know B we can calculate the normal feed velocity V)

$$B=\frac{\rho c V^2 L}{k_0 U}. \quad (30)$$

The conclusion that follows from equation (29) is that the longitudinal flow rate varies linearly with longitudinal position

$$\tilde{Q}=B\xi+C_3. \quad (31)$$

Substituting this result in equation (24) and integrating once in ξ we obtain

$$\tilde{P}=\frac{B}{2I_3(1+\varepsilon,\tau_s)}\xi^2+C_3'\xi+C_4 \quad (32)$$

in which C_3' is a constant that is proportional to the constant C_3 introduced by equation (31). The two constants that appear in equation (32) are obtained next from the conditions that the pressure must be zero at both ends of the contact region

$$\tilde{P}=0 \quad \text{at} \quad \xi=0 \text{ and } 1 \quad (33)$$

and, in the end, equation (32) becomes

$$\tilde{P}=\frac{B}{2I_3(1+\varepsilon,\tau_s)}\xi(\xi-1). \quad (34)$$

The pressure distribution is parabolic, the pressure maximum occurring in the midplane $\xi=1/2$. In other words, the pressure distribution is symmetric about the vertical midplane regardless of whether the base surface moves or remains stationary. From this result we can estimate immediately the total normal force F

$$F=\int_0^L P\,dx \quad (35)$$

which, after using equations (14), (30) and (34), reduces to

$$F=\phi\mu_0\left(\frac{\rho cL}{k_0}\right)^3 V^4. \quad (36)$$

The positive numerical coefficient ϕ is shorthand for the expression

$$\phi=-\frac{1}{12I_3(1+\varepsilon,\tau_s)} \quad (37)$$

which, in principle, is a function of both ε and τ_s. We show in the next section, however, that ϕ is practically independent of ε when the parameter ε becomes much smaller than 1.

Reviewing the ultimate objective of the analysis constructed in this paper, the problem of anticipating the vertical feed speed V is solved as soon as we determine the function ϕ. The solution summarized in equations (36) and (37) shows that the feed speed V is proportional to $F^{1/4}$ and $L^{-3/4}$, in other words, the feed speed V increases when the normal force increases and/or the contact length decreases. The effect of the base surface temperature, τ_s, is conveyed by the coefficient ϕ, which is examined next.

6. RESULTS

The value of the integral I_3 was calculated through a combination of analytical and numerical work. The procedure consisted of first breaking up the right-hand side of equation (26) into two terms

$$I_3(1+\varepsilon,\tau_s)=\int_{1+\varepsilon}^{\tau_s}I_1(\beta,\tau_s)\frac{\beta}{\beta-1}\,d\beta-\frac{I_1(1+\varepsilon,\tau_s)}{I_0(1+\varepsilon,\tau_s)}\int_{1+\varepsilon}^{\tau_s}I_0(\beta,\tau_s)\frac{\beta}{\beta-1}\,d\beta. \quad (38)$$

The second term (the expression preceded by the minus sign) was evaluated analytically for a fixed value of the viscosity exponent n (see the definitions of I_0 and I_1, equations (16) and (17)). The first term on the right-hand side of equation (38) was broken up into a sum of three new integrals by using definition (17)

$$\int_{1+\varepsilon}^{\tau_s}I_1(\beta,\tau_s)\frac{\beta}{\beta-1}\,d\beta=\tau_s\int_{1+\varepsilon}^{\tau_s}\frac{\tau}{\tau-1}\left(\int_\tau^{\tau_s}\frac{\beta^{n+1}}{\beta-1}\,d\beta\right)d\tau-\int_{1+\varepsilon}^{\tau_s}\frac{\tau}{\tau-1}\left(\int_\tau^{\tau_s}\frac{\beta^{n+2}}{\beta-1}\,d\beta\right)d\tau+\int_{1+\varepsilon}^{\tau_s}\frac{\tau}{\tau-1}\eta(\tau,\tau_s)\,d\tau \quad (39)$$

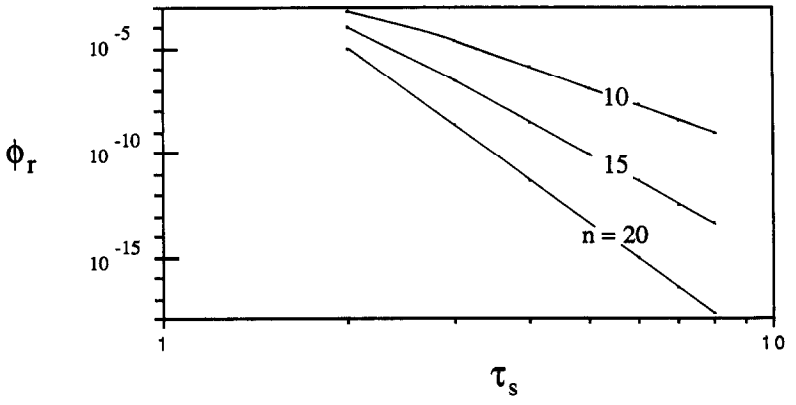

FIG. 4. The effect of the heater surface temperature on the normal feed rate, equations (36) and (37).

where

$$\eta(\tau, \tau_s) = \int_{\tau}^{\tau_s} \frac{\beta^{n+1}}{\beta - 1} \ln\left(\frac{\tau_s - 1}{\beta - 1}\right) d\beta. \qquad (40)$$

The function η and the first two terms appearing on the right-hand side of equation (39) were evaluated analytically. The third term on the right-hand side of equation (39) was evaluated numerically.

Figures 4 and 5 show the way in which ϕ responds to changes in τ_s and ε. First, Fig. 4 shows the 'reference' curve

$$\phi_r = \phi(\varepsilon = 0.01, \tau_s) \qquad (41)$$

which is obtained by assigning to ε the 'small' value of 0.01. The figure houses an entire family of ϕ_r curves because, as illustrated by the calculation procedure in the preceding paragraph, we obtain one ϕ_r vs τ_s curve for each assumed value of the viscosity coefficient n. Generally, the reference coefficient ϕ_r decreases sharply as the base temperature increases. If all the other parameters and properties (e.g. k_0, μ_0) are fixed, this sharp decrease in ϕ_r means also a sharp decrease in the needed normal force (F), or an increase in the feed speed (V), equation (36). These trends make sense, because higher τ_s values mean higher temperatures in the thermal boundary layer, therefore, a runnier layer of softened glass close to the base surface.

Figure 5 measures the relative effect of ε on the function $\phi(\varepsilon, \tau_s)$ by showing how the ratio ϕ/ϕ_r changes as ε passes through the reference value 0.01. The effect of ε is imperceptible when τ_s is of the order of 3 or greater, that is, in the high temperature range required by applications involving the flow of glass (see, e.g. ref. [6]). The figure shows further that the reference value $\varepsilon = 0.01$ is small enough, because ϕ remains practically equal to ϕ_r as ε decreases below 0.01. For this reason, all the velocity and temperature profiles that are described next have been calculated by setting $\varepsilon = 0.01$.

In conclusion, the temperature-dependent coefficient ϕ needed in equation (36) is represented very accurately (within 0.01% at $\tau_s = 3$) by the reference function ϕ_r displayed in Fig. 4. The objective of the analysis—the calculation of F or V—is achieved

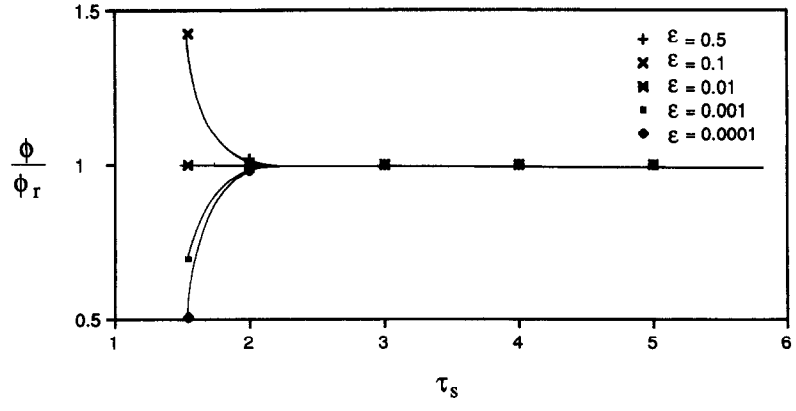

FIG. 5. The insignificant effect of the room temperature limit parameter ε on the results of Fig. 4.

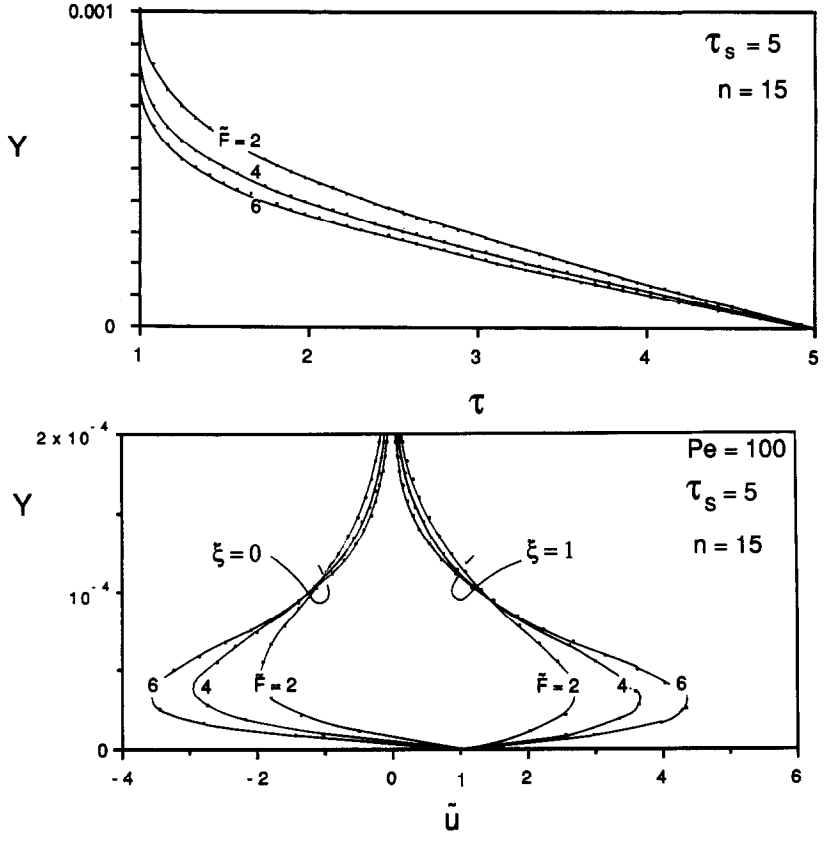

FIG. 6. Temperature and longitudinal velocity profiles when $n = 15$ ($\tau_s = 5$).

by combining equation (36) with the k and μ models (1)–(3) and the information of Fig. 4.

7. THE FLOW AND TEMPERATURE DISTRIBUTIONS

The temperature and velocity profiles of the softened boundary layer can be determined in a straightforward manner after the completion of the numerical work described between equations (38) and (40). For the temperature profile we use equations (6), (9), (37) and (41), to conclude that

$$Y = \phi_r^{1/4}\left[\tau_s - \tau + \ln\left(\frac{\tau_s - 1}{\tau - 1}\right)\right]. \tag{42}$$

In this expression, Y is the dimensionless transversal position referenced to the long side of the boundary layer (L)

$$Y = \frac{y}{L}. \tag{43}$$

As shown in Figs. 6(a) and 7(a), the range occupied by the values of Y is indicative of the true, geometric slenderness ratio of the thermal boundary layer region (note that Y is not the same as $\tilde{y}$). The temperature distribution is nearly linear close to the base surface. Each Y vs τ profile corresponds to a fixed set of values $(n, \tau_s, \tilde{F})$, where $\tilde{F}$ is the dimensionless normal force per unit depth

$$\tilde{F} = \frac{F}{\mu_0 \alpha_0 / L}. \tag{44}$$

The figures show that the boundary layer becomes thinner as the normal force increases. Shifting from Fig. 6(a) to Fig. 7(a), we see that the boundary layer becomes thinner also as the exponent n increases.

The longitudinal velocity profile is obtained by combining equation (21) with the pressure gradient deduced from equation (34)

$$\tilde{u} = \left[I_1(\tau, \tau_s) - I_0(\tau, \tau_s)\frac{I_1(1.01, \tau_s)}{I_0(1.01, \tau_s)}\right] 6\phi_r B(1 - 2\xi) - \frac{I_0(\tau, \tau_s)}{I_0(1.01, \tau_s)} + 1. \tag{45}$$

Worth noting is the relationship between the dimensionless groups B and $\tilde{F}$

$$B = \frac{[-12 I_3(1.01, \tau_s)\tilde{F}]^{1/2}}{Pe} \tag{46}$$

where Pe is the Peclet number defined as

$$Pe = \frac{UL}{\alpha_0}. \tag{47}$$

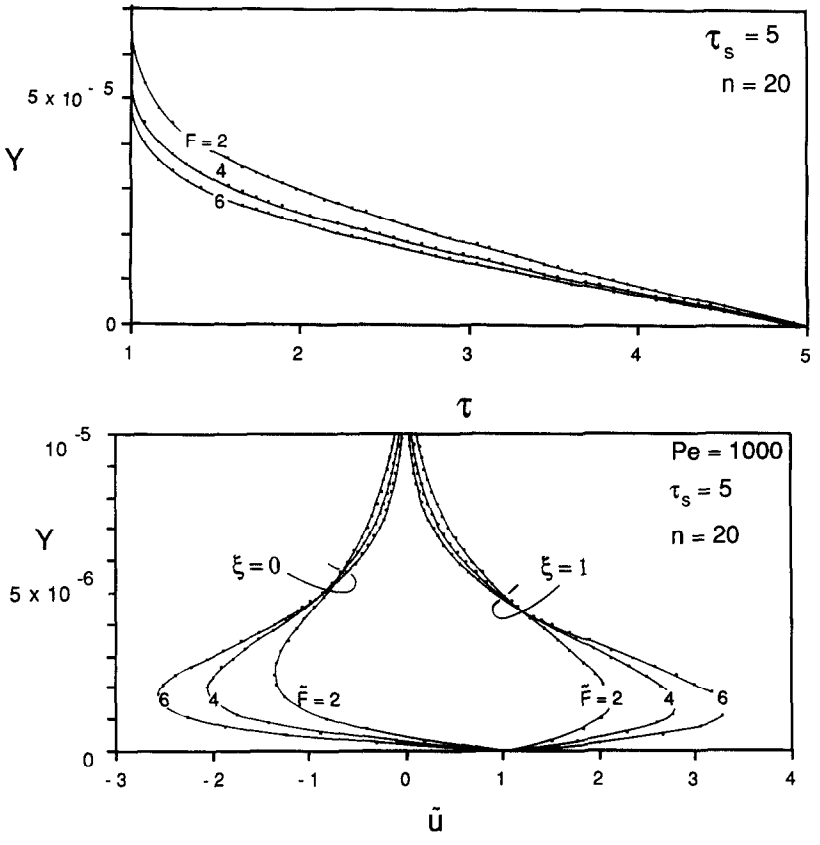

FIG. 7. Temperature and longitudinal velocity profiles when $n = 20$ ($\tau_s = 5$).

The $\tilde{u}$ vs Y curves plotted in Figs. 6(b) and 7(b) were obtained by eliminating τ between equations (45) and (42). These curves show that the longitudinal flow resides in a narrower region than the corresponding thermal boundary layer (compare, e.g. the Y range of Fig. 6(a) with that of Fig. 6(b)). This finding suggests that the longitudinal flow favors the hottest sublayer of the near-base region, that is, the sublayer characterized by the lowest viscosity. Figures 6(b) and 7(b) show further that the flow region becomes narrower and the velocities $\tilde{u}$ increase as the normal force parameter $\tilde{F}$ increases.

8. THE TANGENTIAL FORCE

The net horizontal force experienced by the body of glass as it slides relative to the base surface is

$$F_t = -\int_0^L \left(\mu \frac{\partial u}{\partial y}\right)_{y=0} dx. \tag{48}$$

The force points in the direction of the base surface velocity U (Fig. 1). It can be calculated by using equations (6), (16), (17) and (21), and, omitting the algebra, that final dimensionless expression is

$$\tilde{F}_t = \frac{Pe\,\tilde{F}^{1/4}}{\phi^{1/4} I_0(1+\varepsilon, \tau_s)}. \tag{49}$$

The dimensionless tangential force $\tilde{F}_t$ is defined in the same way as the normal force $\tilde{F}$ of equation (44), namely

$$\tilde{F}_t = \frac{F_t}{\mu_0 \alpha_0 / L}. \tag{50}$$

Figure 8 shows the manner in which $\tilde{F}_t$ depends on the heater surface temperature (τ_s) and the viscosity exponent (n). The quantity plotted on the ordinate is visible also in equation (49): in Fig. 8 the value of ε has been set again equal to 0.01. The figure shows that the tangential force decreases drastically as the heater surface increases, that is, as the 'effective' viscosity of the softened layer decreases. Through the Peclet number, the tangential force is also directly proportional to the relative speed between glass block and heater, U.

The tangential force information can be reported alternatively in terms of the friction factor F_t/F. This alternative can be constructed easily by dividing equations (49) and (44), to conclude that the friction factor decreases and $\tilde{F}^{-3/4}$ as the normal force increases.

9. CONCLUDING REMARKS

Our objective in this paper has been to develop an analytical description of the relationship between mechanical loading and the apparent 'melting' of a block of glass that is pressed against a sliding heater.

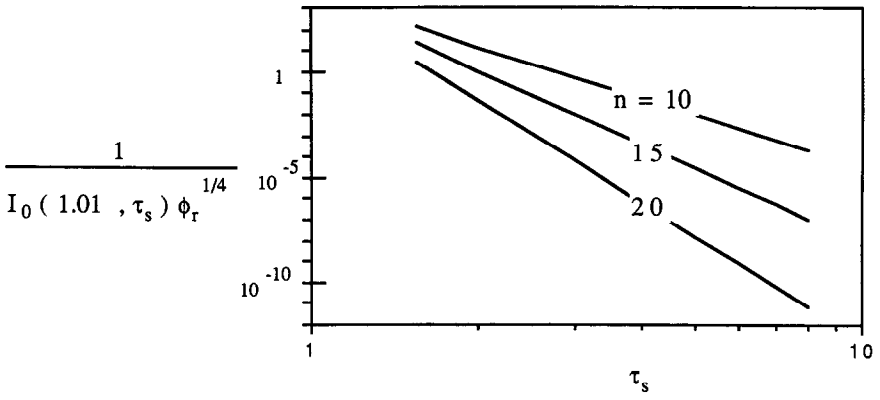

FIG. 8. The effect of the heater surface temperature on the tangential force, equation (49).

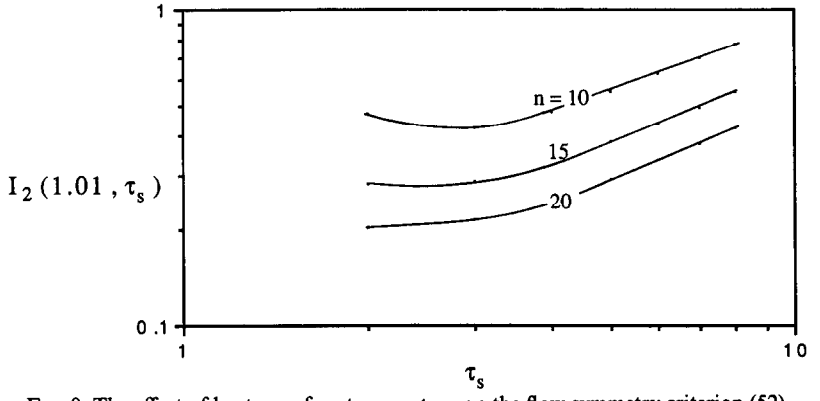

FIG. 9. The effect of heater surface temperature on the flow symmetry criterion (52).

The key results are contained in equation (36) and Fig. 4, and in equation (49) and Fig. 8. These results permit the calculation of the normal feed velocity (V) and the tangential force (F_t), when design parameters such as the normal force (F), the heater temperature (T_s) and speed (U) are known.

Among the simplifying assumptions that made the present analysis workable, the idea that the thermal boundary layer thickness δ does not vary with the longitudinal position is crucial. This assumption is most appropriate when the stagnation (vertical) flow of the softened glass is nearly symmetric about the $x = L/2$ midplane. The degree of symmetry of the boundary layer flow can be tested by comparing the total flow rate of heated glass ($\tilde{Q}_0$) that is being pushed from under the block to the left of $x = 0$, with the flow rate issuing to the right of $x = L$, namely $\tilde{Q}_1$. The flow is nearly symmetric when $\tilde{Q}_0$ is nearly the same as $\tilde{Q}_1$, that is, when the ratio $\tilde{Q}_0/\tilde{Q}_1$ approaches -1. Using equation (24), it is easy to show that

$$\frac{\tilde{Q}_0}{\tilde{Q}_1} = -\frac{B-2I_2}{B+2I_2} \tag{51}$$

which means that $\tilde{Q}_0/\tilde{Q}_1$ approaches -1 when, in an order of magnitude sense

$$B > I_2(1+\varepsilon, \tau_s). \tag{52}$$

Since B varies inversely with U, equation (30), the symmetry criterion unveiled above suggests that U must be smaller than a certain order of magnitude if the softened glass layer is to be nearly symmetric about the midplane $x = L/2$. In the case of no relative motion ($U = 0$) between glass block and heater, of course, the boundary layer region is perfectly symmetric. The values of the integral on the right-hand side of inequality (52) are displayed in Fig. 9.

Acknowledgements—This work was supported by Duke University and the National Science Foundation (Grant No. CBT-8711369). Pedro A. Litsek acknowledges also the support received from his home company Promon Engenharia, S.A.

REFERENCES

1. M. K. Moallemi and R. Viskanta, Analysis of close-contact melting heat transfer, *Int. J. Heat Mass Transfer* **29**, 855–867 (1986).
2. M. K. Moallemi and R. Viskanta, Analysis of melting around a moving heat source, *Int. J. Heat Mass Transfer* **29**, 1271–1282 (1986).
3. B. W. Webb, M. K. Moallemi and R. Viskanta, Experiments on melting of unfixed ice in a horizontal cylindrical capsule, *J. Heat Transfer* **109**, 454–459 (1987).
4. M. Bareiss and H. Beer, An analytical solution of the heat transfer process during melting of an unfixed solid

phase change material inside a horizontal tube, *Int. J. Heat Mass Transfer* **27**, 739–746 (1984).
5. Y. S. Touloukian, R. W. Powell, C. Y. Ho and P. G. Klemens, *Thermophysical Properties of Matter*, Vol. 2. IFI/Plenum, New York (1970).
6. T. Elmer and M. Nordberg, High temperature glasses, *Corning Res.* 225–238 (1961).
7. J. V. Clifton and A. J. Chapman, Natural-convection on a finite-size horizontal plate, *Int. J. Heat Mass Transfer* **12**, 1573–1584 (1969).
8. S. Kimura, A. Bejan and I. Pop, Natural convection near a cold plate facing upward in a porous medium, *J. Heat Transfer* **107**, 819–825 (1985).
9. A. Bejan, The fundamentals of sliding contact melting and friction, *J. Heat Transfer*, to be published.
10. A. Saito, Y. Utaka, M. Akiyoshi and K. Katayama, On the contact heat transfer with melting, *Bull. J.S.M.E.* **28**, 1703–1709 (1985).
11. F. N. Norton, W. D. Kingery *et al.*, USAEC Report NYO-3646, pp. 1–8 (1953).
12. G. K. Batchelor, *An Introduction to Fluid Dynamics*, pp. 219–222. Cambridge University Press, Cambridge (1983).

CHAUFFAGE PAR CONTACT ET ECOULEMENT D'UN BLOC DE VERRE

Résumé—On décrit analytiquement le mécanisme selon lequel un bloc de verre est chauffé, amolli et déformé par contact direct avec une surface solide à température plus élevée. Cette surface peut glisser par rapport au bloc de verre, Celui-ci est modélisé comme un liquide dont la viscosité varie comme T^{-n} ou T est la température absolue et n un nombre du domaine 10–20. Les distributions de température et de vitesse dans la couche mince de verre chaud (mou) sont déterminées. Des procédures de calcul simple sont développées pour la vitesse de déformation du bloc de verre et pour la relation générale entre les forces exercées sur le bloc, le transfert thermique et le phénomène de lubrification qui gouverne le mécanisme de déplacement du verre.

KONTAKT-HEIZUNG UND GLEITSTRÖMUNG AN EINEM GLASKÖRPER

Zusammenfassung—Es wird der Vorgang analytisch beschrieben, bei dem ein Glaskörper aufgeheizt, erweicht und erodiert wird durch den direkten Kontakt mit einer festen Oberfläche höherer Temperatur. Diese Oberfläche kann sich relativ zum Glaskörper bewegen. Das Glas wird als Flüssigkeit beschrieben, dessen Viskosität proportional zu T^{-n} ist, wobei T die absolute Temperatur und n eine Zahl im Bereich zwischen 10 and 20 ist. Es werden Temperatur- und Geschwindigkeitsverteilungen in der dünnen, heißen, angeschmolzenen Glasschicht bestimmt. Es werden einfache Berechnungsgleichungen angegeben für den Zustand, bei dem der Glasblock erodiert wird, sowie für die Abhängigkeit zwischen den auf den Block wirkenden Kräften und dem kombinierten Wärmeübergangs- und Gleitphänomen, durch den der Glasabtrag bestimmt wird.

КОНТАКТНЫЙ НАГРЕВ И ПЛАСТИФИЦИРОВАННОЕ ТЕЧЕНИЕ СТЕКЛЯННОГО ТЕЛА

Аннотация—Аналитически описывается процесс нагрева, размягчения и разрушения (плавления) стеклянного тела при прямом контакте с твердой поверхностью со значительно более высокой температурой. Эта поверхность может скользить относительно стекляного тела. Стекло моделируется жидкостью, вязкость которой изменяется как T^{-n}, где T—абсолютная температура, а n—число, изменяющееся в диапазоне от 10 до 20. Определены распределения температуры и скорости в тонком слое нагретого (мягкого) стекла. Разработаны простые расчетные методики для определения скорости разрушения стеклянного бруска, а также общей зависимости между действующими на брусок силами и совместными теплопереносом и явлением пластификации, определяющими процесс удаления стекла.